Light Metals 2014
Edited by: John Grandfield
TMS (The Minerals, Metals & Materials Society), 2014

A NOVEL HEAT RECOVERY TECHNOLOGY FROM AN ALUMINUM REDUCTION CELL SIDE WALLS: EXPERIMENTAL AND THEORETICAL INVESTIGATIONS

Yaser Mollaei Barzi[1], Mohsen Assadi[1], Håvard Møllerhagen Arvesen[2]
[1]Faculty of science and technology, University of Stavanger, 4036 Stavanger, Norway
[2]Goodtech Recovery Technology AS, Per Krohgs Vei 4, 1065 OSLO, Norway

Keywords: Aluminum reduction cell, Heat recovery, Heat pipe, Two-phase loop thermosyphon, Ledge profile

Abstract

In this study, a comprehensive experimental and theoretical investigation is carried out aiming to develop an efficient and effective heat recovery technology from an Aluminum smelter side lines. The influences of the heat recovery system on the cell operation and side line ledge profile are also investigated in this paper. The experimental setup consists of an electrical furnace which provides the simulated hot side walls, the control and measurement instruments, the heat recovery unit, the cooling system, etc. The heat recovery unit is an externally insulated two-phase loop thermosyphon designed and manufactured specifically for this purpose which is capable of extracting heat from the hot plate actively with very high performance. In addition, a simple smart mathematical model is developed for the heat recovery unit (Heat Pipe) and aluminum smelter side lines accounting for the dynamic ledge profile variations and phase change. Using the developed model, the heat recovery strategy and also the possible and applicable alternatives for the side walls heat collection and utilization system are investigated considering system flexibility and self-adjustment ability.

Introduction

Since the Hall-Heroult process was invented in 1886, there has been continuously a progress trend towards larger production units and higher productivity along with lower specific energy consumption. All major companies have carried out extensive projects to increase the amperage in existing potlines (capacity creep) aiming to improve specific energy consumption of the reduction cells. Concern about the energy consumption in production of primary aluminum has led to interest in recovery and utilization of the excess heat in the process.

Currently, efficient smelters consume roughly 13 MWh of electricity per ton of aluminum, while roughly half of that energy is lost as thermal waste as heat. From the total wasted heat, approximately 25 to 35 % is dissipated through the cell side walls depending on the cell design and geometry [1]. According to a case study accomplished by Nowicki and Gosselin, side walls of the aluminum smelters are the second largest heat dissipation source in a primary aluminum production plant after pot line exhaust gas [1]. In spite of the huge amount of available waste heat in this process, the possibility of thermal integration and utilization still faces some several challenges. The low quality of the waste heat (i.e., low temperature) and some practical process complexities are the main reasons impeding waste heat recovery and thermal integration in aluminum smelters. Moreover, the availability of waste heat and demand for heat in a heat utilization system is difficult to be synchronized due to the transient behavior of the heat transfer processes. In addition, the thermal balance and maintaining the adequate protective layer of frozen bath at the sidelining are of primary concerns which should be fulfilled and guarantied with any proposed heat recovery solution.

Despite existing challenges on on-site implementation of a heat recovery and utilization system for aluminum electrolysis cells, several relevant patents and publications have been already recorded. Newer patents comprise cooling by placing heat exchangers in the cell wall [2, 3] as well as active cooling of the anode yokes [4]. The other inventions reported for waste heat recovery from different primary aluminum production processes are listed in references [5-7]. Ladam et al. [8] investigated three main heat sources of an aluminum cell and different alternatives for the utilization system. In the analysis performed by Ladam et al. it was found that electric power corresponding to 0.33 kWh/kgAl could be obtained from a heat exchanger at the outside of the cell side walls. Likewise, Nowicki et al. [1] reviewed the opportunities for waste heat recovery and thermal Integration in the primary aluminum industry highlighting the challenges and proper solutions either in new plant design or existing plant modification. In addition, Lavoie et al. [9] tried to expand the power modulation window of Aluminum smelter pots by controlling the heat dissipation from aluminum smelting pot shells using an air cooled shell heat exchanger technology. They stated that their heat extraction system enables a fast readjustment of the cell heat balance by controlling the heat loss from the shell, suitable to counter-balance major power input variation to the cell. This study focuses on the viability and possibility of actively extracting the waste heat dissipated from side walls of an Aluminum smelter. The aim is primarily to enhance the thermal balance and ledge profile controllability and adjustability and secondarily to increase the energy efficiency of the system by recovering wasted heat via a heat utilization system. Extracting the waste heat (capturing it in a heat transfer fluid) requires adapted heat exchanger designs. In addition, a very compact design is needed to use the solution also for retrofitting and up-grading existing production cells. The safety aspect is a further main topic as installations are close to high current and molten material. A high performance two-phase loop thermosyphon heat exchanger has been designed and adapted to be attached to the cell side walls transferring the extra heat to the thermal oil circuit. The system flexibility and self-adjustment ability are the main issues which have to be investigated precisely for such an application. For this purpose, the detail behavior of the aluminum cell and heat extraction system as well as the thermosyphon heat exchanger is investigated at different operating conditions using a simple-smart mathematical model. The extent of the self-adjustment capability, the power extraction versus working temperature characteristics and efficiency are the issues we are going to predict and specify in this study.

Heat recovery system configuration and principals

The main idea of the heat recovery technology is to place heat collection units at the outside of the pot shell. The collection units are based on the heat pipe (thermosyphon) principle and include the thermosyphon and the insulation layer attached behind it.

They are connected in parallel piping system and the heat is removed using thermal oil. The heat is collected by passing thermal oil through the condenser at the top of the thermosyphons to be used in an energy utilization system. The thermal oil is Paratherm NF with the optimum temperature range of about 40 °C to 340 °C [10]. The principals of the proposed heat recovery system for an aluminum reduction cell are shown schematically in Fig. 1.

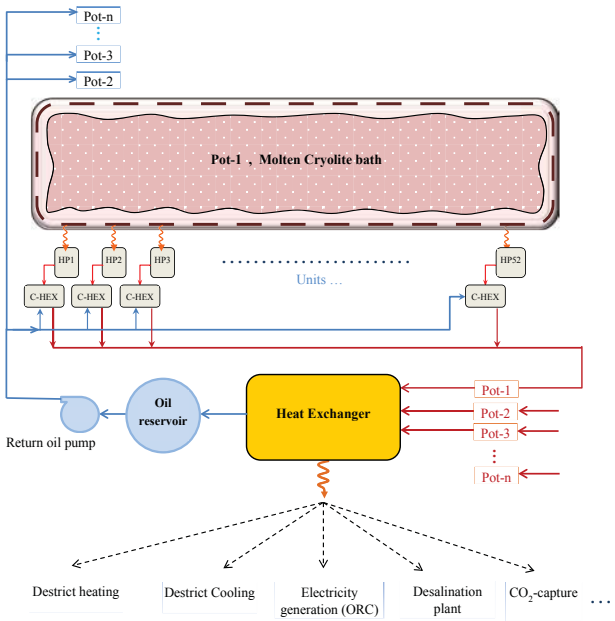

Figure 1. Principals of the proposed heat recovery technology for an Aluminum reduction cell

The assembly is flexible enough to avoid problems related to any probable pot shell deformation. The designed thermosyphon behavior has been examined experimentally and theoretically in whole range of the desired operating condition and its functionality has been proven [11].

Thermosyphon design aspects and laboratory tests

The thermosyphon heat pipes are known as very high performance heat transfer devices. The principle of the thermosyphon heat pipes is well proven. A thermosyphon heat pipe consists of a sealed pipe containing a two phase working fluid. The incoming heat (at the bottom of the pipe) evaporates the liquid. By removing heat at the top of the closed pipe the vapor condenses, and the liquid flows back to the bottom of the pipe by gravity. Since evaporation and condensation take place at the same temperature, the temperature of the pipe will be practically uniform. The temperature can be lowered by increasing the flow of thermal medium through the condenser at the top, which increases the heat flow into the evaporation region, and vice versa. The system will, therefore, to a large degree be self-regulating. For the proposed heat extraction unit application, a specific design of the thermosyphon has to be adapted to fulfill the desired thermal and geometrical requirements. To evaluate the thermosyphon's behavior for aluminum reduction cell's heat recovery application, a laboratory scale test setup is devised to simulate aluminum cell side wall thermal conditions as a heat source using an electrical furnace (Figure 2). The furnace provides the heat source in the form of a vertical hot plate with the surface area of about 60×60 cm^2 and the temperature range of 100 to 1100°C. Several designs with shape and dimensions suitable for mounting between the cradles on a pot shell have been extensively tested in the laboratory, and the final results are very promising.
The thermosyphon evaporator section is designed as flattened-bed straight pipes which cover mostly the hot plate surface to absorb maximum possible heat from the plate. The vapor is collected from the evaporator tubes using the top horizontal collector pipe. The condenser section is a horizontal pipe which is finned externally and surrounded by a concentric jacket to be cooled by an oil flow through the oil jacket. The inlet oil mass flow rate and temperature are adjustable parameters; however the oil outlet temperature depends on the evaporator temperature and general performance of the thermosyphon. The temperature is measured and recorded in different points of the thermosyphon using temperature sensors brazed to the heat pipe wall. The total thermal power effect of the thermosyphon is calculated using the data of the condenser mass flow rate and inlet and outlet oil temperature.

Figure 2. Thermosyphon assembly test setup at the Goodtech laboratory [11]

Heat extraction unit and cell side line dynamic model

To investigate preliminarily the cell response to the heat extraction system, a simple dynamic heat transfer model is developed. The model is based on the equivalent thermal resistances of the side line elements and the ledge profile (Fig. 3).

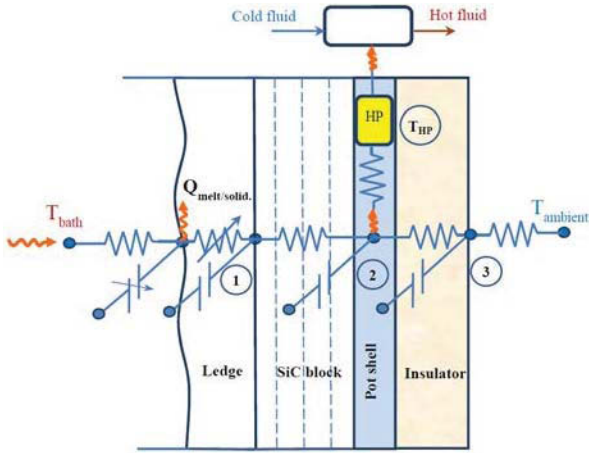

Figure 3. Thermal elements across the side wall

As shown in the figure, an equivalent electrical circuit is considered to simulate the heat conduction and heat absorption throughout the different system elements. The thermal resistances consist of the ledge profile, the pot side walls, the heat pipe walls and the insulator conduction resistances and liquid bath and air heat convection resistances. To take the transient behavior of the

system in to account, the thermal capacitors are assigned to each element which is representative of its dynamic heat absorption or extraction capacity. For the ledge profile, a variable resistor and capacitor is considered due to the ledge variable thickness around the bath. As depicted in the figure, the excess heat from the bath is absorbed mainly by the heat pipe and the rest is conducted to the air through the insulator. The heat pipe is treated as a heat sink which delivers the extracted heat to the oil flow via the condenser. A heat sink/source is considered at the solid-liquid contact area due to the latent melting/solidification heat of the ledge. The model shown in Fig. 1 is further developed for a 2-D or 3-D heat transfer analysis based on the accuracy and detail level requirements.

The thermal properties and geometrical parameters of the cell side line heat transfer media is defined based on a typical cell case study (Table 1, 2). The height of the available area for heat recovery unit is assumed to be 60 cm. In addition, the bath super heat and the ambient temperature are provided as inputs and presented in Table 2. The bath superheat is assumed to vary in range of 5 to 12 °C in different operating conditions.

Table I. Geometrical parameters and properties of the cell side line heat transfer media [12]

	Thickness (cm)	Surface area (cm2)	Density (kg/m3)	Heat capacity (J/kg K)	Thermal conductivity (W/m K)
Ledge	Variable	60 × 60	2850	1850	1.07
Sic block	7.6	60 × 60	3100	750	40
Metal shell casing (A36 grade)	2	60 × 60	8000	486	45
Insulator	1.5	60 × 60	1500	500	0.04
Heat pipe casing + contact	0.5	60 × 60	N/A	430	15

Table II. Thermal conditions of the bath and heat recovery unite [13]

Bath superheat range (°C)	5-12
Ledge melting enthalpy (kJ/kg)	520
Ambient temperature (°C)	25
Bath thermal convection coefficient (W/m^2K)	1450
Air thermal free convection coefficient (W/m^2K)	25

Ledge profile model

The total heat conducted through the bath in to the side walls is calculated by the following equation.

$$\dot{Q}_{in} = h_{bath} A\left(T_{bath} - T_{melting\ point}\right) \quad (1)$$

h_{bath} is the bath liquid heat convection coefficient which is dependent on the bath heat transfer conditions and composition. It can be found in some literatures [13]. Equation (2) describes the heat balance in the node located on the leading edge of the ledge profile.

$$\dot{Q}_{melt} = \dot{Q}_{in} + G_{ledge}(T_1 - T_{melt}) \quad (2)$$

The phase change heat sink/source is calculated with equation (3) in which h_{sl} is the latent melting/solidification heat for the ledge material and $\frac{dl_{ledge}}{dt}$ is the ledge profile thickness variation rate.

$$\dot{Q}_{melt} = \rho_{ledge} A\, h_{sl}\, \frac{dl_{ledge}}{dt} \quad (3)$$

The sign of $\dot{Q}_{melt}$ depends on the ledge profile (l_{ledge}) variation (decreasing or increasing) which is interpreted to a heat sink (negative value of $\dot{Q}_{melt}$) or a heat source (positive value of $\dot{Q}_{melt}$) respectively in this point. The variable heat conductance and capacitance of the ledge are calculated by following equations.

$$G_{ledge} = \frac{k_{ledge}\, A_{ledge}}{L_{ref} - l(t)} \quad (4)$$

$$C_{ledge} = \rho_{ledge}\, A(L_{ref} - l(t)) c_{ledge} \quad (5)$$

Side wall's heat transfer media model

The heat transfer media of the cell side walls contains of: ledge profile, SiC block (the pot side wall material), metal casing, heat pipe and insulator. Following equations are drawn for the heat transfer media components which describe their dynamic heat transfer behavior. The heat balance equation written for each node leads to a set of differential equations with unknown variables: $T_1(t)$, $T_2(t)$, $T_{HP}(t)$, $T_3(t)$, $l_{ledge}(t)$.

$$C_{ledge}\frac{dT_1}{dt} = G_{ledge}(T_{melt} - T_1) + G_{SiC}(T_2 - T_1) \quad (6)$$

$$C_{SiC}\frac{dT_2}{dt} = G_{SiC}(T_1 - T_2) + G_{steel}(T_{HP} - T_2) + G_{Ins}(T_3 - T_2) \quad (7)$$

$$C_{HP}\frac{dT_{HP}}{dt} = G_{Steel}(T_2 - T_{HP}) - \dot{Q}_{HP} \quad (8)$$

$$C_{Ins}\frac{dT_3}{dt} = G_{Ins}(T_2 - T_3) + G_{conv}(T_{amb} - T_3) \quad (9)$$

Equation (8) describes the heat balance in the heat pipe node and $\dot{Q}_{HP}$ is the power duty of the thermosyphon heat pipe. Generally, the heat pipe duty is not only affected by its surrounding media temperature (T_{HP}), but also by the heat pipe characterizations and specifications. To solve the set of differential equations, we need to have a function describing the heat pipe behavior besides the other elements. We expect such a function $\dot{Q}_{HP}(T_{HP}, T_{in,Oil}, \dot{m}_{Oil})$ for the heat pipe duty definition which is also dependent on the cooling oil flow conditions. The model proposed to simulate the heat pipe behavior is described in next section.

Thermosyphon mathematical model

The thermosyphon behavior is formulated using a set of one-dimensional conservation equations of momentum, heat and mass transfer describing the steady state operation of a vertically oriented and gas loaded loop thermosyphon. The heat transfer model consists of a one-dimensional axial heat transfer equation in which the radial heat exchanges are considered by the

equivalent wall thermal resistances. In addition the returning liquid profile and the liquid level variation at the bottom of the thermosyphon (stationary liquid) are taken in to consideration in the model. Following assumptions have been made for the model to avoid long computational time and high cost compromising with the accuracy and reality-coincidence of the model.

- One dimensional heat, mass and momentum transport processes in the axial direction
- Thermal equilibrium between the working fluid and its surrounding wall [14]
- Treatment of non-condensable gases as a perfect gas

The set of equations are solved numerically via discretization of the equations over the geometrical domain. Figure 4 depicts the geometrical model of the thermosyphon. As shown in Figure 4, the geometrical domain is divided into a number of differential elements and centered nodes that represent the local discrete values of the variables. Each thermosyphon node is connected to an external node within a thermal resistor which represents the thermosyphon radial heat transfer either in the evaporator or the condenser sections. Detailed description of equations and computational method used to solve the equations are extensively presented in reference [15]. The model results and the equivalent experimental data are shown in Figures 5 and 6 as the total thermal power handling capability of the thermosyphon and the oil outlet temperature respectively versus the thermosyphon temperature and the oil mass flow rate. According to Figure 5, the thermal power handling capability of the thermosyphon depends on both evaporator temperature and oil mass flow rate.

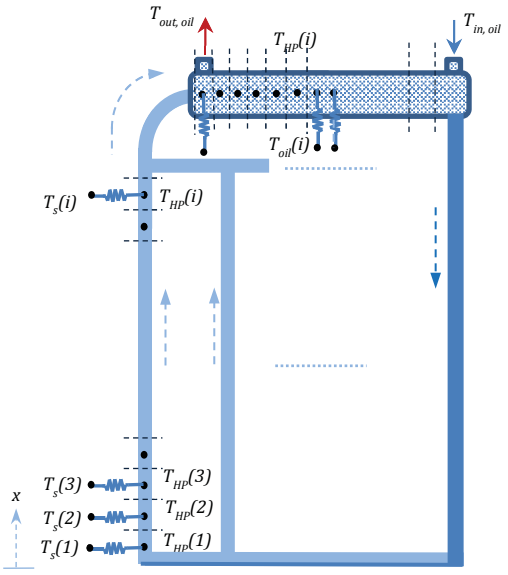

Figure 4. Geometrical model used for the loop heat pipe numerical simulation

For the minimum oil mass flow rate of 50 kg/hr, the thermosyphon thermal power effect is in the range of 1 to 4.8 kW for the evaporator temperature range of 140 to 300 °C. This thermal power effect can be increased to a maximum of 8.2 kW by increasing the oil mass flow rate to 150 kg/hr. The oil mass flow rate affects the heat transfer capability of the condenser by affecting the oil flow convection heat transfer coefficient due to the oil flow velocity and Reynolds number variation. The more condenser heat transfer capability is the higher thermal power extraction from the hot plate is achieved. However, in high mass flow rates (more than 125 kg/hr) and consequently high oil velocities, the oil mass flow rate has less influence on the convection heat transfer coefficient of the oil.

Almost the same trend is observed for the oil outlet temperature versus the evaporator temperature as shown in Figure 6. The oil outlet temperature decreases when the oil mass flow rate increases, especially in high mass flow rates, even though more heat is extracted from the hot plate. The oil temperature increases almost 55 to 85 °C depending on the oil volumetric flow rate when it is passing through the condenser.

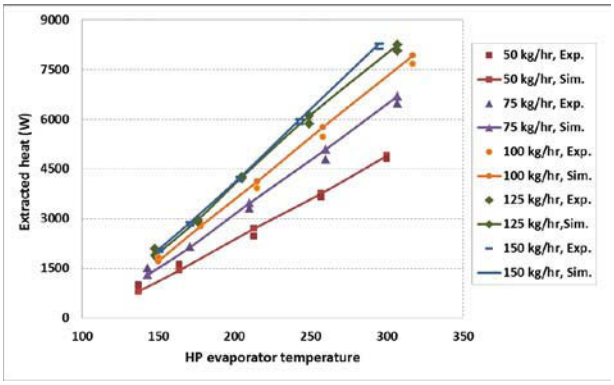

Figure 5. The thermosyphon thermal power effect predicted by the model and the experimental data in different oil flow rates

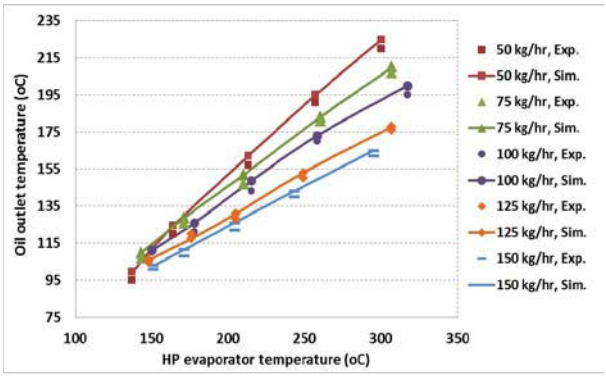

Figure 6. The oil outlet temperature predicted by the model and the experimental results versus the evaporator temperature

The cell side line dynamic response to the heat extraction unit

The cell response to the heat extraction unit application and also effects of some concerning input parameters are investigated using the developed model. For this purpose, equations (1) to (9) are solved numerically using a Matlab code. The thermosyphon thermal power handling effect ($\dot{Q}_{HP}(T_{HP}, T_{in,Oil}, \dot{m}_{Oil})$) is calculated using the thermosyphon model as a Matlab function.

The pre-defined concerning events examined by the model are listed below and their major effects on the cell operation are presented in Table 3.

1: Ordinary operation of the cell (steady state, bath super heat of 7 °C)

2: Attaching the heat recovery system to the side walls (base case: Oil flow rate of 175 lit/hr and inlet oil temperature of 85 °C)

3: Decreasing the thermal oil flow rate (in 3 steps, 125 lit/hr, 75 lit/hr and 50 lit/hr)

4: Bath super heat increase (7 to 8 °C in oil flow rate of 125 lit/hr)

5: Bath super heat decrease (8 to 6 °C in oil flow rate of 125 lit/hr)

6: Detaching the insulation from the unit

In addition, the dynamic variation of temperature and the ledge profile thickness versus time is depicted in Figures 7 and 8 respectively. According to the results, the steady state condition of the cell is predicted and located at the time axis origin. At this point the ledge thickness is 5.2 cm and the cell side wall temperature is 431 °C based on the pot shell specifications and material properties presented in Tables 1 and 2.

Table III. Subsequent cell events associated with heat recovery system and the cell response

	1	2	3	4	5	6
SiC internal temperature (Hot side, ^{o}C)	455	173	189 212 244	202	176	455
Side wall outside temperature	431	140	158 182 214	156	150	431
Insulator cold side temperature	-	37	38.5 41 44	39.5	37.6	-
Ledge thickness (cm)	5.1	8	7.8 7.7 7.2	6.8	9.39	5.1
Available heat (extracted, kW)	-	184	183.8 189.9 181.2	210	157	-

As shown in Figure 7, the sidewall temperature drops sharply when the heat extraction unit is mounted at the cell sidewalls and it reaches to around 150 °C in new steady state condition. Furthermore, it can be seen from Figure 8 that the ledge profile thickness increases up to 8.1 cm due to the new side wall heat transfer mechanism.

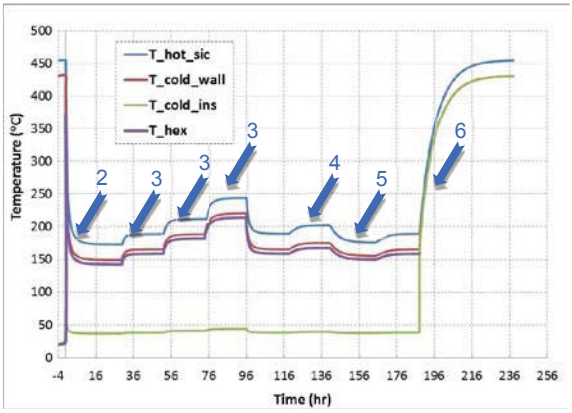

Figure 7. Time variation of temperature in the cell side line

It is assumed that the unit is being cooled by the oil flow rate of 175 lit/hr at the beginning of the process. Then the effect of changing the coolant fluid flow rate is investigated within a three-step reduction of the oil flow rate. The oil flow rate drop results in the side wall temperature increase in three stages and consequently melting the ledge until the thickness of 7.32 cm at minimum oil flow rate.

The other issue investigated by the model is the consequences of the bath temperature fluctuations and its effect on the heat extraction unit and the cell side line ledge. The system response to the bath temperature variation shows that the heat extraction unit is able to be well-adapted to the cell internal parameters variation. According to the data presented in Table 3, the extracted heat increases about 30 kW when the bath super heat increases 1 °C. Reversely when the bath super heat drops 2 °C, the absorbed heat reduces about 53 kW. As shown in Figure 8, 2 °C of bath superheat variation causes just 1.3 cm ledge thickness variation out of about 7 cm total thickness. Moreover, the average response time of the system to the input perturbations is calculated more than 12 hours as shown in figures 7 and 8.

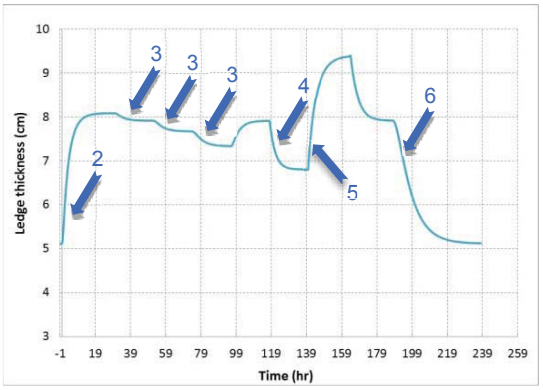

Figure 8. Time variation of the ledge thickness in the cell side line

Since breakdown may be experienced in any technical system including proposed heat recovery system some solution has to be devised for such emergency cases. Hence, there will be a safety system that will prevent any damage of the cell in such conditions so that the heat can be lost in other ways. Automatic application/removal of thermal insulation is part of the strategy for emergency cases and increased power modulation. This scenario has been examined by the model through which the insulation removal effects are investigated. Case 6 in Figure 7 and 8 shows the temperature and side ledge thickness variation respectively due to the insulation removal. It can be observed from the figure that the removal of the insulator will result in the system to turn back gradually to the normal condition in about 15 hours.

Heat utilization system estimation and evaluation

In the proposed heat recovery system, a number of above mentioned heat extraction units are mounted to the Aluminum cell outside walls to extract the waste heat. The absorbed heat is conducted to the oil flow passing through the individual condensers and the hot oil is collected to be used in an energy conversion system. As shown in Figure 1, different alternatives could be proposed potentially for the heat utilization system. To be able to realistically evaluate and adapt the proper heat utilization system we have to precisely define the output parameters range of the heat extraction system. Table 4 gives some output parameters range of one cell heat extraction system based on the presumed operating condition.

Table IV. Output parameter's range of one cell sidewall heat extraction system

Parameter	Range
Oil mass flow rate (kg/hrs.)	Min: 50 (One unit) Max: 175 (One unit)
One cell thermal power output (kW)	Min: 140 (at 5°C bath superheat) Max: 315 (at 12°C bath superheat)
Hot oil temperature (°C)	Min: 110 (max oil flow rate) Max: 200 (min oil flow rate)

Piping system pressure drop (bars, one cell)	Min: 0. 1 (50 kg/hr oil flow, 8°C bath superheat) Max: 0.96 (175 kg/hr oil flow, 5°C bath superheat)

In case of implementation of heat recovery system for several aluminum cells, the total extractable thermal power could be simply calculated by multiplying the heat from one cell to the number of the cells. However the available hot oil temperature is almost the same as the value given in Table 4. Likewise, the pressure drop doesn't vary too much in a parallel piping concept, even though the mass flow rate should be multiplied by the number of the cells. For example, for a pot line with 100 cells the scale of the available heat will be average 20000 kW. Based on the temperature range and available amount of heat, different types of energy conversion systems are eligible for this application including district heating, cooling (absorption chillers), ORC electrical power generation, desalination plant etc. However, a comprehensive techno-economical study is necessary to decide which solution is most profitable and effective considering the particular cell design, number of incorporated cells, plant layout and nearby available facilities.

In this study we are going to focus on the heat recovery possible solution for one cell to investigate and demonstrate the main heat recovery idea. Among different utilization systems, the ORC cycle is recognized to be more feasible for demonstration purpose and technology applicability study. The organic working fluid used in ORC cycles allows Rankin cycle to utilize the heat from lower temperature sources such as industrial waste heat. The low-temperature heat is converted into useful work that can itself be converted into electricity. Considering the heat source temperature varying from 110 to 200 °C, the ORC is therefore perfectly adapted for this kind of application. However, it is important to keep in mind that the efficiency depends strongly on heat sink temperature (defined by the ambient temperature). If we want to be rather conservative in our assumptions 10% efficiency is reasonable for proposed heat recovery case. It means that the net available power output will be in range of 14 to 31 kW for the cell and heat recovery system studied in this paper.

To adapt a proper ORC cycle to the proposed thermal integration system with aforementioned operating range, another research study is being accomplished, by present authors, in which the detail design aspects and equipment specifications will be investigated and defined.

Conclusion

A novel active cooling system for extracting the excess heat from sidewalls of an Aluminum reduction cell was investigated using the thermosyphon heat pipe technology. A specific thermosyphon design was adopted practically for this purpose and it's functionality for such an application was well-proved through the laboratory test results. Furthermore, a mathematical simulation method was adopted for the heat extraction unit including the ledge profile, sidewall heat transfer media and thermosyphon models. The model results give the preliminary image of the cell response to the proposed heat extraction system implementation as well as the net recoverable heat from the cell. Also, the heat extraction system capability, to be adjusted with the cell different operating modes, is theoretically examined. The heat utilization system can be designed conceptually based on the data available by the present model. Several options are possible for heat utilization purpose although a careful feasibility analysis is necessary to decide which measure is the most profitable. The ORC cycle application for the available extracted heat was proposed for demonstration of one cell heat recovery functionality. There is a need for further research into adapting an ORC heat utilization system and required elements in detail level based on available temperature and thermal power ranges.

Acknowledgments

Financial support of this work by NFR (Research Council of Norway) and the laboratory test facilities provided by the Goodthech Recovery AS, Norway are gratefully appreciated.

References

1. C. Nowicki, L. Gosselin, "An overview of opportunities for waste heat recovery and thermal integration in the primary aluminum industry", Journal of the Minerals, Metals and Materials Society, 64(8) (2012), 990-996.
2. J. A. Aune, K. Johansen and P. O. Nos, "Electrolytic Cell for the Production of Aluminium and a Method for Maintaining a Crust on a Sidewall and Recovering Electricity", WO/2001/94667.
3. O.J. Siljan, "Electrolysis Cell and Structural Elements to be Used Therein", WO/2004/083489.
4. B.P. Moxnes and A. Solheim, "Method and Means for Control of Heat Balance", WO/2006/088375.
5. E. Næss, , T. Slungaard, , O. Sønju, and B.P. Moxnes, "A Method and Equipment for Heat Recovery", WO/2006/009459.
6. H.K. Holmen and S. Gjørven, "A Method and a System for Energy Recovery and/or Cooling", WO/2006/031123.
7. J.A. Aune, and P.O. Nos, "Method for Controlling the Temperature of Components in High Temperature Reactors", WO/2002/39043.
8. Y. Ladam, A. Solheim, M. Segatz and O.A. Lorentsen, "Heat recovery from aluminium reduction cells" (Paper presented at the Minerals, Metals & Materials Society conference, Light Metals, San Diego, California, 2011), 393.
9. P. Lavoie, S. Namboothiri, M. Dorreen, J. J. J. Chen, D. P. Zeigler and M. P. Taylor, "Increasing the power modulation window of aluminum smelter pots with shell heat exchanger technology" (Paper presented at the Minerals, Metals & Materials Society conference, Light Metals, San Diego, California, 2011), 369.
10. Paratherm NF Heat Transfer Fluid, brochure by Paratherm.
11. S. Teie, "Loop Heat Pipe characteristics and performance analysis", Oslo laboratory, Goodtech Recovery Technology AS, Apr. 2013.
12. M. P. Tailor, W. D. Zhang, V. Wills and S. Schmid, "A dynamic model for the energy balance of an electrolysis cell", Trans IChemE, 74(A) (1996), 913-933.
13. A. Solheim, "Some aspects of heat transfer between bath and side ledge in aluminum reduction cells", (Paper presented at the Minerals, Metals & Materials Society conference, Light Metals, San Diego, California, 2011), 381.
14. G. A. S. Glover, "An Analysis of the Performance of a Vertically Oriented, Gas Loaded, Variable Conductance Heat Pipe" (MSc thesis, Monterey, California Naval Postgraduate School, 1986).
15. Y. Mollaei Barzi, M. Assadi, "experimental and Theoretical investigation of a loop heat pipe/thermosyphon behavior in a heat recovery system application" (Paper accepted for presentation in 17th International Heat Pipe Conference, Kanpur, India, October 16 2013).